Flow Behavior of a Gas−Liquid−Solid Fluidized Bed in a Self-Circulating Operation through an External Conduit

Nobuyuki Hidaka,* Kazuhiro Kakoi, and Toshitatsu Matsumoto

Department of Applied Chemistry and Chemical Engineering, Kagoshima University, Kagoshima 890, Japan

Flow behavior of liquid and multicomponent mixtures of solid particles in fluidizing columns with an external conduit was investigated for a self-circulating operation by an airlift effect. Experimental and analytical results are presented for circulating rates of liquid and particles and for axial changes in holdups of gas and solid in the column. From good agreement between both results, it was found that a one-dimensional sedimentation−dispersion model and mechanical energy balance equation were successfully applied to predict the axial change in gas and solid holdups as well as the circulating rates of liquid and solid particles in the columns.

Introduction

An airlift bubble column with or without suspended solid particles is an important technique for contacting gas and liquid (or slurry) and is particularly used in fermentation industries. The airlift bubble column is one of the modified bubble columns, and a pool of liquid or slurry is divided into two vertical zones connected at the top and bottom. When gas is sparged at the bottom of one of these zones, the difference of bulk density between the gas-sparged zone and the unsparged zone induces liquid (or slurry) circulation. The zone in which gas and liquid flow upward concurrently is called the "riser", and the other zone where gas and liquid flow downward concurrently is called the "downcomer". There are two types of airlift bubble columns. One of these types of which the downcomer is located internally to the riser is known as an internal-circulation-loop airlift, whereas it is known as an external-circulation-loop airlift where the downcomer is located externally to the riser.

Many works (Kubota et al., 1978; Hsu and Dudukovic, 1980; Merchuck and Stein, 1981; Bello et al., 1984; Jones, 1985; Popovic and Robinson, 1987a,b, 1989; Chisti et al., 1988) have been published on the flow behavior in airlift bubble columns with or without suspended solid particles, but most were restricted to the case of those in the bubble column with an internal loop. Herskowitz and Merchuk (1986) investigated the hydrodynamics of a three-phase fluidization with an external conduit by using three particle types of 1.7−8.6 mm in diameter, porous and nonporous, spheres and cylinders. However, they conducted the experiments for batchwise operation with respect to solid particles. In a self-circulating operation through an external conduit, very little information is available on the behavior of individual solid particles in a column whose contents is a mixture of particles widely different in diameters.

In the present study, a mixture of sieved glass beads was fluidized in vertical columns in a self-circulating operation through an external conduit by using an airlift effect. Axial distributions of solid holdup of each component in the column and the circulating rates of liquid and solid particles were investigated experimentally and compared with a simulation based on a sedimentation−dispersion model for the solid dispersion in the bed and on mechanical energy balances for the circulation of slurry.

Experimental Apparatus and Procedure

A schematic diagram of the experimental setup for the gas−liquid−solid three-phase fluidization is shown in Figure 1. The fluidization column, constructed from an acrylic resin pipe, having an inner diameter of 7 cm and a height of 4.50 m, was placed in a vertical position. A side tube, 7 cm diameter and 10 cm length, for the outlet of solid particles was attached horizontally at a height of 4.14 m from the bottom. The external conduit, made of a poly(vinyl chloride) resin pipe with an inner diameter of 1.9 cm and a height of 3.95 m, was connected with the fluidization column at the bottom, by which a self-circulation of slurry owing to an airlift effect was produced. To receive the discharge of liquid and solid particles from the fluidization column, a divergent section was provided at the top of the external conduit. The other geometric dimensions of the apparatus are indicated in Figure 1 and are listed in Table 1.

The local solid holdup, defined as the volume fraction of particles suspended in a unit volume of slurry in the column, was measured by using a shutter method (Al-Dibouni and Garside, 1979; Matsumoto et al., 1989, 1991, 1992; Hidaka et al., 1992, 1993, 1995a,b). Twenty shutter plates, made of a 3-mm-thick stainless steel plate, were installed horizontally at 0.2-m intervals and were interconnected with a wire rope. The fluidization column was sectioned instantaneously by pulling the rope. The gas tightness was assured with O-rings which are attached on each cross section of the column wall. The column, 15 cm in diameter and 2.7 m in height, was equipped with 11 shutter plates, and the other features were fundamentally the same as those of the 7-cm-diameter column. The gas distributor was a spiral copper tube and was the same as that of previous works (Matsumoto et al., 1989, 1991, 1992).

Air and tap water at approximately 20 °C were used for the gas and liquid phases. Sieved glass beads of 244, 277, and 489 μm diameter and mixtures thereof were used for the solid phase. Their physical properties and size distributions are shown in Table 2 and Figure 2, respectively. After the bed was continuously operated for approximately 0.5 h, all shutter plates were simul-

S0888-5885(97)00353-9 CCC: $15.00
Published on Web 01/05/1998

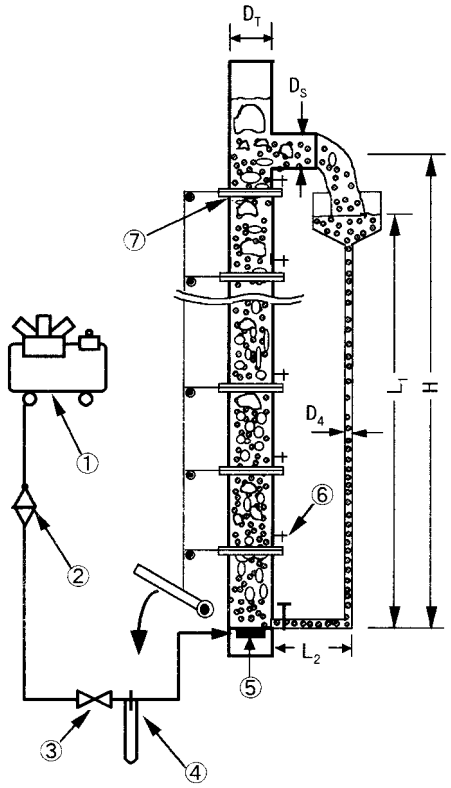

Figure 1. Schematic diagram of the experimental apparatus: (1) compressor; (2) oil−mist separator; (3) valve; (4) orifice meter; (5) gas distributor; (6) solid withdrawal tap; (7) shutter plate.

Table 1. Geometric Dimensions of the Experimental Apparatus

diameter (m)			length (m)		
D_T	D_s	D_4	H	L_1	L_2
0.07	0.07	0.019	4.14	3.95	0.30
0.15	0.094	0.05	2.65	2.43	0.18

Table 2. Properties of Glass Beads and Parameters

d_p (μm)	ρ_p (kg/m^3)	v_t (m/s)	Ga	n, eq 29
244	2500	0.028	214	2.87
277	2500	0.034	312	2.76
489	2500	0.071	1720	2.38

taneously closed by stopping the feeds of gas and liquid. The column was momentarily partitioned into 21 portions for the 7-cm-diameter column or 12 portions for the 15-cm-diameter column by this action. The local value of solid holdup of each component in the slurry phase, ϕ_{pi}, was determined by weighing the particles trapped in each plate. The mean gas holdup was calculated from the total volume of gas in each section.

Circulating Rate of Liquid

The circulating liquid velocity in the external conduit is affected by the gas velocity, the mass of solid particles suspended in the bed, and the geometric dimensions of the apparatus. Figure 3 illustrates the control volumes by which the mechanical energy balance was taken. The equations are

for section 1−2

$$\rho_1 gh = (1/2)\rho_2 \langle v_2 \rangle^2 + \rho_2 E_{v1} \qquad (1)$$

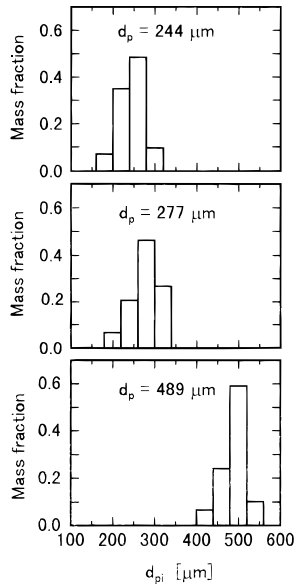

Figure 2. Size distribution of solid particles used.

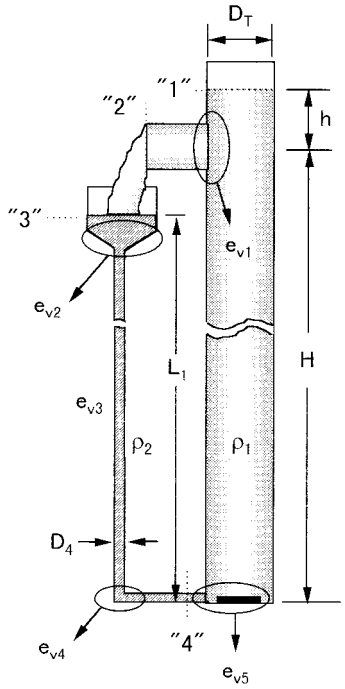

Figure 3. Schematic representation of control volumes for mechanical energy balance.

for section 3−4

$$P_3 - P_4 = (1/2)\rho_2\langle v_4\rangle^2 - \rho_2 g L_1 + \rho_2(E_{v2} + E_{v3} + E_{v4}) \qquad (2)$$

for section 4−1

$$P_4 - P_1 = -(1/2)\rho_2\langle v_4\rangle^2 + \rho_1 g(H + h) + \rho_1 E_{v5} \qquad (3)$$

where $\langle v \rangle$ is the liquid velocity, averaged over a cross section, and P_1 and P_3 are the atmospheric pressures. E_{v1} is the friction loss per unit mass of fluid due to the discharge at plane 2, E_{v2} to the contraction at the divergent section of external conduit, E_{v3} to the straight tube, E_{v4} to the bend, and E_{v5} to the expansion at the bottom of the column. E_v for each section is evaluated by introducing a friction loss factor, e_v, defined as

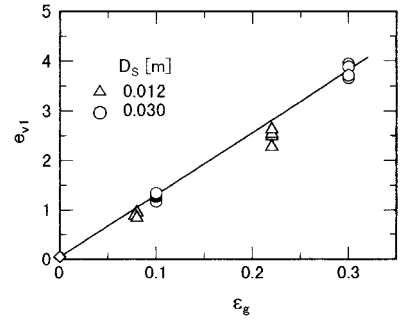

Figure 4. Correlation of e_{v1}.

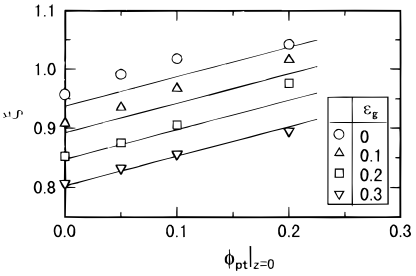

Figure 5. Correlation of ξ.

Table 3. Friction Loss Factors

obstacles	e_v
contraction	$e_{v2} = (32/3\alpha)(1/Re)\{(D_4/D_3)^3 - 1\}$ where α is a diffuser angle, being 60° for the present system
straight tube	$e_{v3} = 4(L/D)f$; $f = 0.0791Re^{-1/4}$
elbow	$e_{v4} = 0.8$

$E_v/(\langle v\rangle^2/2)$. ρ_1 is the apparent density of the gas−liquid−solid mixture in the bed, and ρ_2 is that in the external conduit.

$$\rho_1 = \rho_g\epsilon_g + \rho_l\epsilon_l + \rho_p\epsilon_p = \{\rho_l(1 - \bar{\phi}_{pt}) + \rho_p\bar{\phi}_{pt}\}(1 - \epsilon_g) \quad (4)$$

$$\rho_2 = \rho_l(1 - \bar{\phi}_{pt}) + \rho_p\bar{\phi}_{pt} \quad (5)$$

where $\bar{\phi}_{pt}$, is the average value of ϕ_{pt}. If ϵ_g, $\bar{\phi}_{pt}$, and e_v are known, the value of $\langle v_4\rangle$ is determined from eqs 1−3. For the gas−liquid−solid flow, however, no reliable information was reported on E_{v1} or e_{v1} and E_{v5} or e_{v5}. As shown in Figure 4, e_{v1} was experimentally obtained by applying eq 1. The value of e_{v1} increased with increasing ϵ_g and was correlated as

$$e_{v1} = 12.57\epsilon_g + 0.054 \quad (6)$$

The friction loss factor e_{v5} expressed by

$$e_{v5} = \{\xi(D_T/D_4)^2 - 1\}^2 \quad (7)$$

where ξ is a correction factor. The value of ξ was determined experimentally from the pressure loss between plane 4 and the inside of the column at the same horizontal position, as shown in Figure 5, and the following equation was obtained.

$$\xi = -0.45\epsilon_g + 0.5\phi_{pt}|_{z=0} + 0.937 \quad (8)$$

The other friction loss factors which were used in the calculation of circulating liquid velocity are conventional ones, as listed in Table 3. Using the continuity equation for liquid, the linear liquid velocity at $z = 0$, $u_l|_{z=0}$ and the superficial liquid velocity, U_l, in the column, respectively, are given as follows:

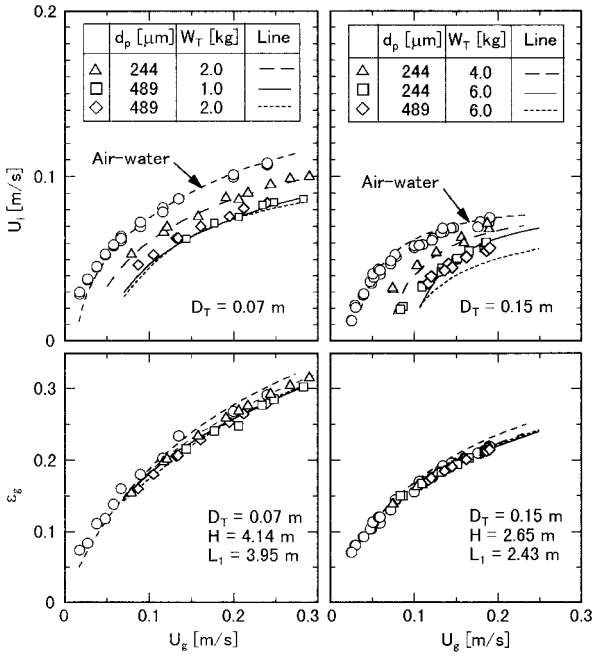

Figure 6. Experimental and calculated results of the circulating rate of liquid and gas holdup.

$$u_l|_{z=0} = \frac{\rho_2}{\rho_l}\left(\frac{D_4}{D_T}\right)^2 \frac{\langle v_4\rangle}{(1 - \epsilon_g)(1 - \phi_{pt})} \quad (9)$$

$$U_l = u_l|_{z=0}(1 - \epsilon_g)(1 - \phi_{pt}) = \langle v_4\rangle\left(\frac{\rho_2}{\rho_l}\right)\left(\frac{D_4}{D_T}\right)^2 \quad (10)$$

Figure 6 shows the experimental and calculated results of circulating liquid velocity and gas holdup in the main column. The experimental value of U_l was determined by measuring the liquid flow rate at the outlet of the column. The calculated values of U_l and gas holdup are obtained from eqs 1−3 and 21 by approximating that $\rho_2 = \rho_l$. The results are in good agreement with the data.

Modeling of Axial Change in Solid Holdup

As reported by Matsumoto et al. (1992), it was difficult to find a set of ϕ_{pi} values, which were required in order to start the calculation of the steady-state material balance equations in the case of a multicomponent mixture of solid particles. Thus, we used conveniently the unsteady-state material balance equations, in conjunction with arbitrary initial conditions, satisfying the material balance for the total mass of *i*-particles in the column. The steady-state solution for *i*-particles was then obtained as an asymptotic solution when the axial distribution of ϕ_{pi} was constant with time, which was developed for the batch operation with respect to solid particles by Matsumoto et al. (1992) and Hidaka et al. (1992, 1995b). This was also used for the present circulating operation with an external conduit.

The unsteady-state material balance equations of *i*-particles in the column and external conduit are respectively given by

in column
$$\frac{\partial \phi_{pi}}{\partial t} + \frac{\partial}{\partial z}\left[u_{pi}\phi_{pi} - E_{pi}\frac{\partial \phi_{pi}}{\partial z}\right] = 0 \quad (11)$$

in external conduit
$$\frac{\partial \phi_{pi}}{\partial t} + \frac{\partial}{\partial z}[u_{pi}\phi_{pi}] = 0 \quad (12)$$

The initial condition is given by

$$t \le 0; \qquad \phi_{pi}(0,z) = \phi_{pi0}(z) \quad (13)$$

where ϕ_{pi0} is an arbitrary function that satisfies the following equation.

$$W_i = \frac{\pi D_T^2}{4}\int_0^H \phi_{pi}\rho_p(1-\epsilon_g)\,dz + \frac{\pi D_4^2}{4}\int_0^L \phi_{pi}^*\rho_p\,dz \quad (14)$$

The first and second terms on the right-hand side of eq 14 are mass of *i*-particle in the column and that in the external conduit, respectively. The boundary conditions at inlet and outlet are

$$z = 0; \qquad u_{pi}\phi_{pi} - E_{pi}\frac{\partial \phi_{pi}}{\partial z} = u_{pi}\phi_{pi}^* \quad (15)$$

$$z = H; \qquad u_{pi}\phi_{pi} - E_{pi}\frac{\partial \phi_{pi}}{\partial z} = K_{pr}\phi_{pi} \quad (16)$$

where ϕ_{pi}* in eqs 14 and 15 is the solid concentration of *i*-particles at the inlet of the column. $K_{pr}\phi_{pi}$ in eq 16 is the effluent of solid particles from the outlet of the column and is predicted by the following equation (Hidaka et al., 1995a).

$$K_{pr}\phi_{pi} = \frac{U_l}{(1-\epsilon_g)}\frac{1}{3(1-\epsilon_g)}\phi_{pi} \quad (17)$$

Other important parameters and factors are as follows:

(i) Time-Averaged Linear Velocity of *i*-Particles. The time-averaged linear velocity of *i*-particles with respect to the fixed coordinate at an axial position z is denoted as

$$u_{pi} = u_l - u_{ti} \quad (18)$$

where u_{ti} is the settling velocity of the *i*-particles in a quiescent fluid. u_l is the linear velocity of the liquid and is related to the superficial liquid velocity as

$$u_l = U_l/[(1-\epsilon_g)(1-\phi_{pt})] \quad (19)$$

(ii) Circulating Rate of Solid Particles. The total circulating rate of solid particles for components $1-N$ is derived from eq 16 (Hidaka et al., 1 995a).

$$W_r = \sum_{i=1}^{N} W_{ri} = \frac{\pi D_T^2}{4}\sum_{i=1}^{N} K_{pr}(1-\epsilon_g)\phi_{pi}|_{z=H}\rho_p \quad (20)$$

(iii) Estimation and Correlation Equations of Parameters ϵ_g, E_{pi}, u_{ti}. The parameters used in the model calculation have been correlated by Matsumoto et al. (1992) as follows:

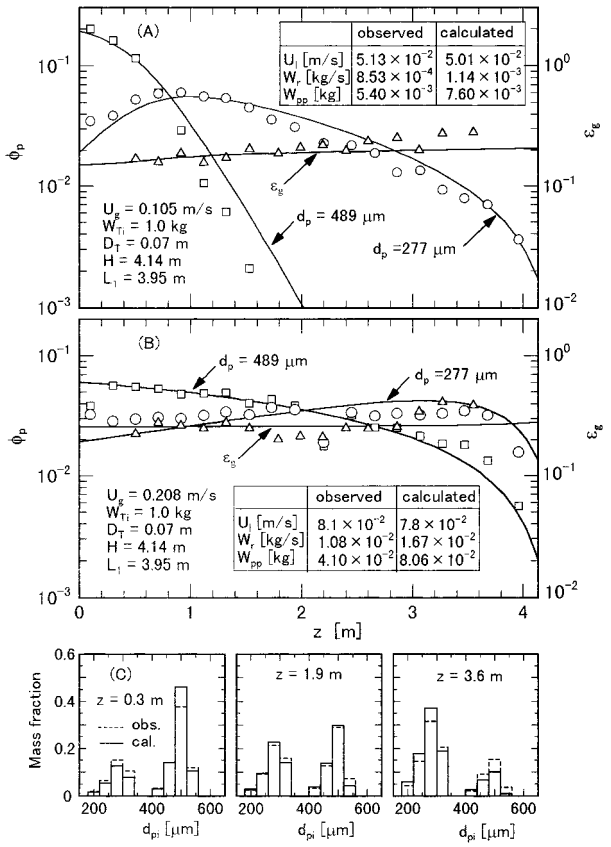

Figure 7. Effect of gas velocity on axial changes for a mixture of glass beads of 277 and 489 μm diameter in a 7-cm-diameter column: (A) axial distributions of gas and solid holdups at U_g = 0.105 m/s; (B) axial distributions of gas and solid holdups at U_g = 0.208 m/s; (C) size distribution of solid particles at *z* under the same experimental conditions as part B. Solid lines are calculated by assuming four components by size for each glass beads. Symbols: solid holdup, ○, d_p = 277 μm, □, d_p = 489 μm; gas holdup, △.

(a) The local gas holdup for gas−liquid−solid systems:

$$\epsilon_g = U_g(1-R)/\{0.29(1+2.5\phi_{pt}^{0.85}) + cU_g(1-R)\} \quad (21)$$

where $R = \epsilon_g U_l/[(1-\epsilon_g)U_g]$. The constant *c* in eq 21 is 1.8 for D_T = 0.07 m and 2.4 for D_T = 0.15 m. The solid lines of the gas holdup shown in Figures 7A,B and 8A are calculated from eq 21.

(b) The axial dispersion coefficient of *i*-particles:

$$E_{pi} = \sum_{i=1}^{N} E_{pi0}\phi_{pi}/\phi_{pt} \quad (22)$$

where the contribution of different components is taken into account by the volume fraction of each monocomponent. E_{pi0} is the axial dispersion of *i*-particles alone and is related to the axial dispersion coefficient of liquid for the air−water system, E_l, by the following equation.

$$E_{pi0}/E_l = 1 - 0.01Re_i^{*2/3} \quad (23)$$

Equation 23 is valid for $Re_i^* = d_{pi}[\epsilon_g(1-R)(gD_T/2)]^{1/2}/\nu < 500$. The axial dispersion coefficient of liquid is

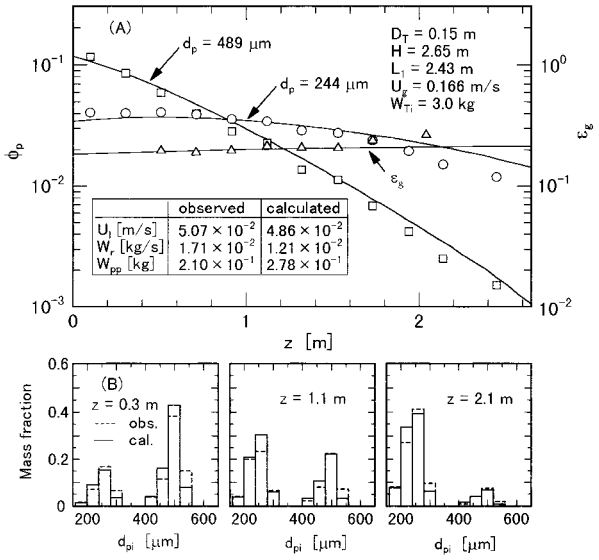

Figure 8. Experimental and calculated results for a mixture of glass beads of 244 and 489 μm diameter at $U_g = 0.166$ m/s in a 15-cm-diameter column: (A) axial distributions of gas and solid holdups; (B) size distribution of solid particles. Solid lines are calculated by assuming four components by size for each glass beads. Symbols: solid holdup, ○, $d_p = 244$ μm, □, $d_p = 489$ μm; gas holdup, △.

expressed by

$$\frac{E_l}{(gD_T^3)^{1/2}} = \left\{\left[\frac{k[\epsilon_g(1-R)]^{1/2}}{1-\epsilon_g}\right]^3 + 0.09^3\right\}^{1/3} \quad (24)$$

for $D_T = 0.07$ m, $\quad k = 0.3[1 + 4U_l/(1-\epsilon_g)]$

for $D_T = 0.15$ m, $\quad k = 0.3$

(c) The slip velocity between i-particles and liquid velocity:

$$d_{pi}u_{ti}/\nu = Re_{ti} = Re_{\infty i}F_i \quad (25)$$

where $Re_{\infty i}$ is defined by $v_{\infty i}d_{pi}/\nu$, based on the settling velocity of isolated i-particles, $v_{\infty i}$, and F_i is a voidage function. According to Matsumoto et al. (1989, 1992), $Re_{\infty i}$ is given by

$$Re_{\infty i} = \frac{Ga_i\zeta_i}{[18^{4/5} + (Ga_i\zeta_i/3.0)^{2/5}]^{5/4}} \quad (26)$$

where

$$\zeta_i = 1 + \left\{\frac{6.5[\epsilon_g(1-R)]^{1/2}Ga_i^{1/3}}{1 + \{[\epsilon_g(1-R)]^{1/2}Ga_i^{1/3}/15\}^2}\right\}^{3/2} Ga_i^{-2/3} \quad (27)$$

In three-phase fluidized beds, the voidage function of Richardson-Zaki (1954) cannot be applied (Matsumoto et al., 1989), and the following equation for multicomponent systems has been proposed (Matsumoto et al., 1992) as

$$F_i = \{(1-\phi_{pt})[1 - (\phi_{pt}/\phi_{pc})^3]^{1/3}\}^{n_i-1}\prod_{j=1}^{N}\{(1-\phi_{pj}) \times [1 - (\phi_{pj}/\phi_{pc})^3]^{1/3}\}^{n_j-n_i} \quad (28)$$

where ϕ_{pc} is the correction factor equal to 0.55 and n_i is given as follows:

$$(n_i - 2)/(5 - n_i) = 6.0Ga_i^{-1/2} \quad (29)$$

Procedure of Numerical Calculation

Equations 11−16 were transformed into the dimensionless forms using the following variables below:

$$T = tU_l/H, \quad Z = z/H, \quad u^*_{pi} = u_{pi}/U_l, \quad E^*_{pi} = E_{pi}/(U_lH) \quad (30)$$

The equations were then rewritten in finite difference forms, in which the upwind-difference approximation (Gosman et al., 1969) was applied to the convection term in eq 11. Next, a set of nonlinear tridiagonal equations derived was solved numerically. Grid sizes were fixed as $\Delta Z = 0.025$ and $\Delta T = 0.01$ in the present computation. The convergence criterion at each grid point was given as $(\phi_{pi}^{j+1} - \phi_{pi}^{j})/\phi_{pi}^{j} < 0.01$. The steady-state solution for i-particles is obtained as an asymptotic solution when the axial distribution of ϕ_{pi} remains unchanged with time. Details of this calculation have been published elsewhere (Matsumoto et al., 1992; Hidaka et al., 1992, 1995b).

Results and Discussion

Axial Distribution of Solid Particles and Particle Size Distribution at z in the Column. Figure 7A shows axial changes in gas and solid holdups for a mixture of glass beads of 277 and 489 μm diameter in the 7-cm-diameter column. Each component of glass beads, of which the amount was 1.0 kg, was fluidized simultaneously at $U_g = 0.105$ m/s. The holdup of larger particles decreases monotonously with an increase in the axial position, but the holdup of smaller particles shows a convex profile and takes a maximum value in the axial position. For a higher gas velocity than that of Figure 7A, the axial profile of solid holdup was flatter and a high holdup zone of smaller particles moved upward due to the increases of circulating liquid velocity and axial mixing of solid particles, as indicated in Figure 7B. As a result, both component glass beads were circulated through the external conduit. Figure 7C shows the measured size distribution of solid particles at several positions of z. The experimental conditions were the same as those in Figure 7B. As can be seen, the mass fraction of smaller particles gradually increased with an increase in the axial position.

Figure 8 shows the results of axial changes and size distribution in the 15-cm-diameter column where a mixture of glass beads of 244 and 489 μm diameter were fluidized at $U_g = 0.166$ m/s. Since axial mixing in this column is much larger than that in the 7-cm-diameter column, the solid holdup distribution becomes flatter compared with that in the 7-cm-diameter column at a similar gas velocity condition.

The solid lines in Figures 7A,B and 8A indicate the calculated axial changes in gas and solid holdups. In the numerical calculations, the glass beads with average diameters of 244, 277, and 489 μm were divided into four components by particle size ($i = 4$), as shown in Figure 2. The experimental data are well estimated by the calculation. The measured and calculated circulating rates of liquid and solid particles are also shown in these figures. The calculated particle size distribution

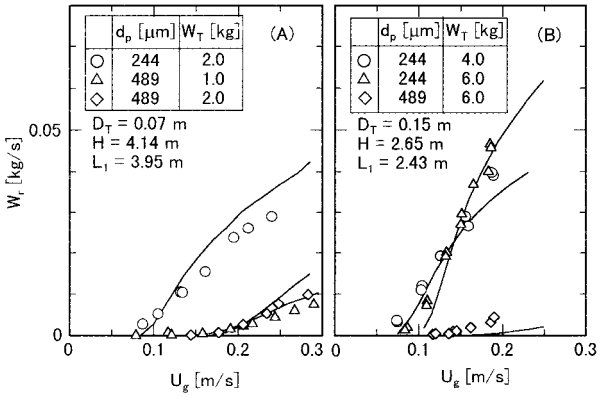

Figure 9. Experimental and calculated results of the circulating rate of solid particles for a monocomponent system.

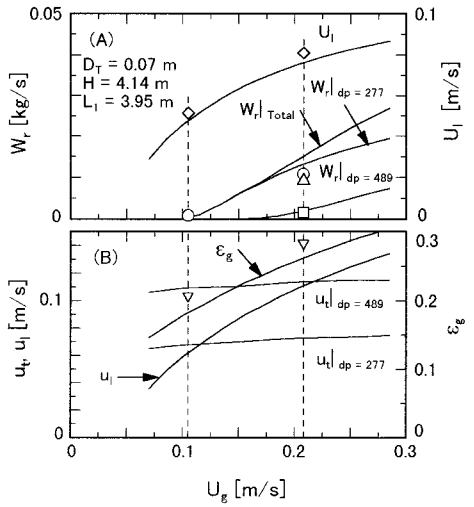

Figure 10. Effect of gas velocity on the circulating rates and slip velocity between the *i*-particles and liquid for a mixture of glass beads of 277 and 489 μm diameter in a 7-cm-diameter column, of which the amount is 1.0 kg for each component.

at an arbitrary height in the column was obtained from the calculated axial changes of *i*-component solid holdup. Agreement between the calculated and measured size distributions is satisfactory, as shown in Figures 7C and 8B.

Circulating Rate of Solid Particles. Figure 9 shows the circulating rate of solid particles for the monocomponent system, measured under the same conditions of particle size and amount of particles as those in Figure 6. The circulating rate increases with increasing gas velocity and amount of fluidized particles and decreases with increasing particle diameter. Solid lines in the figure are calculated from eq 20, by using parameters correlated by eqs 21−29, and agreed well with the data.

Figure 10A shows the effect of gas velocity on circulating rates for a mixture of 277- and 489-μm-diameter glass beads when 1.0 kg of each component was fluidized in the 7-cm-diameter column. The solid lines are the calculated results. The axial change in solid holdup is caused by the interaction between gravitational settling and turbulent mixing of solid particles due to the bubbles. If the effect of diffusive flux (turbulent mixing) on the circulating rate of solid particles is not dominating, the *i*-component particles are circulated as in eq 18 when the linear liquid velocity, u_l, is larger than the slip velocity of particles, u_{ti}. The relationship between u_l and u_{ti}, being evaluated from the average solid holdup

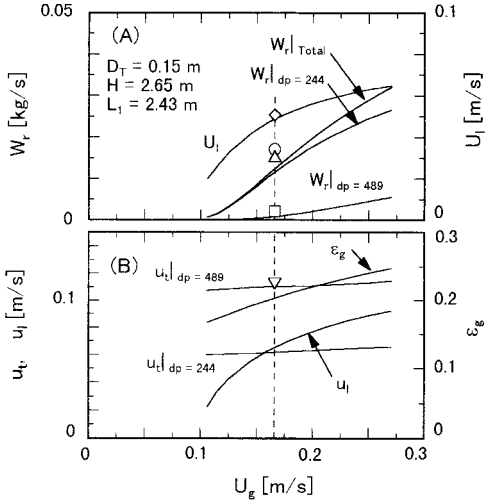

Figure 11. Effect of gas velocity on the circulating rates and slip velocity between the *i*-particles and liquid for a mixture of glass beads of 244 and 489 μm diameter in a 15-cm-diameter column, of which the amount is 3.0 kg for each component.

in the column, is indicated in Figure 10B. The dotted lines correspond to the experimental and calculated results under the conditions of parts A and B of Figure 7, respectively. Thus, it is possible to predict whether *i*-component particles circulate or not under a given set of operating conditions. Figure 11 shows the effect of gas velocity on the circulating rates in the 15-cm-diameter column, for the case in which the amount is 3.0 kg for each component. The dotted line in the figure corresponds to the results under the condition of Figure 8.

Conclusion

In a gas−liquid−solid fluidized bed containing a mixture of solid particles of different diameter, the axial distributions of gas and solid holdups in the column were measured in a self-circulating operation with an external conduit. The circulating rates of liquid and solid particles in the external conduit were also measured in the case of the self-circulating operation. A calculation, based on the sedimentation−dispersion model for the solid dispersion, eqs 11 and 12, and mechanical energy balances for the circulation of slurry, eqs 1−3, was in good agreement with the experimental data. Parameters in the model were correlated with empirical equations.

Nomenclature

D_s = diameter of side outlet tube for slurry effluent, m
D_T = diameter of column, m
D_4 = diameter of external conduit, m
d_p = average diameter of particles, m
d_{pi} = diameter of *i*-particles, m
E_v = friction loss per unit mass, J/kg
e_v = friction loss factor defined by $e_v = E_v/(\langle v\rangle^2/2)$
E_l = axial dispersion coefficient of liquid, m^2/s
E_{pi} = axial dispersion coefficient of *i*-particles, m^2/s
E_{pi}* = dimensionless axial dispersion coefficient of *i*-particles defined by $E_{pi}/(U_l H)$
F_i = voidage function in eq 25
f = friction factor
Ga_i = modified Galilei number of *i*-particles defined as $d_{pi}^3 g(\rho_p/\rho_l - 1)/\nu^2$
g = gravitational acceleration, m/s^2

H = distance from bottom of column to side-tube outlet, m
h = distance from side-tube outlet to surface of liquid in column, m
K_{pr} = averaged effluent velocity, m/s
k = correction factor appearing in eq 24
L = length of external conduit, m
L_1 = vertical distance from inlet of column to liquid level in head tank installed at top of external conduit, m
L_2 = horizontal distance of external conduit at inlet of column, m
n_i = exponent in eq 28
R = dimensionless parameter defined by $\epsilon_g U_l/(1 - \epsilon_g)U_g$
Re_∞ = Reynolds number defined by $d_p v_\infty/\nu$
Re_t = Reynolds number defined by $d_p u_t/\nu$
Re_i* = Reynolds number defined by $d_{pi}\{\epsilon_g(1 - R)(gD_T/2)\}^{1/2}/\nu$
T = dimensionless time defined by tU_l/H
t = time, s
U_g = superficial velocity of gas, m/s
U_l = superficial velocity of liquid, m/s
u_l = linear velocity of liquid, m/s
u_{pi} = linear velocity of i-particles with respect to fixed coordinate, m/s
u_{pi}* = dimensionless linear velocity of i-particles defined by u_{pi}/U_l
u_{ti} = slip velocity between u_l and u_{pi}, m/s
v_t = terminal settling velocity of a solid particle in quiescent liquid, m/s
v_∞ = effective settling velocity of solid particles in three-phase systems, m/s
W_{pp} = mass of particles in external conduit, kg
W_{ri} = circulating rate of i-particles, kg/s
W_r = circulating rate of particles defined by W_{ri}, kg/s
Z = dimensionless axial distance from gas distributor defined by z/H
z = axial distance from gas distributor, m

Greek Letters

ϵ_g = gas holdup
ζ_i = correction factor appearing in eq 26
ν = kinematic viscosity of liquid, m^2/s
ξ = correction factor appearing in eq 7
ρ_l = density of liquid, kg/m^3
ρ_p = density of solid particles, kg/m^3
ϕ_{pc} = correction factor in eq 28
ϕ_{pi} = holdup of i-particles in slurry
ϕ_{pt} = total solid holdup, $\sum\phi_{pi}$

Subscripts

i = component of particles
$i0$ = monocomponent i-particles
t = total

Literature Cited

Al-Dibouni, M. R.; Garside, J. Particle Mixing and Classification in Liquid Fluidized Beds. *Trans. Inst. Chem. Eng.* **1979**, *57*, 96−103.

Bello, R. A.; Robinson, C. R.; Moo-Young, M. Liquid Circulation and Mixing Characteristics of Airlift Contactors. *Can. J. Chem. Eng.* **1984**, *62*, 573−577.

Chisti, M. Y.; Halard, B.; Moo-Young, M. Liquid Circulation in Airlift Reactors. *Chem. Eng. Sci.* **1988**, *43*, 451−457.

Gosman, A. D.; Pun, W. A.; Runchal, A. K.; Spalding, D. B.; Wolfshtein, M. *Heat and Mass Transfer in Recirculating Flows*; Academic Press: London, 1969; Chapter 3.

Herskowitz, M.; Merchuck, J. C. A Loop Three-Phase Fluidized Bed Reactor. *Can. J. Chem. Eng.* **1986**, *64*, 57−61.

Hidaka, N.; Onitani, M.; Matsumoto, T.; Morooka, S. Axial Mixing and Segregation of Multicomponent Coarse Particles Fluidized by Concurrent Gas−Liquid Flow. *Chem. Eng. Sci.* **1992**, *47*, 3427−3434.

Hidaka, N.; Masuda, T.; Matsumoto, T.; Morooka, S. Transient Behavior of the Vertical Distribution of Solid Holdup with a Step Change in Liquid Velocity in a Long Bubble Column. *Ind. Eng. Chem. Res.* **1993**, *32*, 1588−1591.

Hidaka, N.; Kakoi, H.; Matsumoto, T.; Morooka, S. Transient Discharge of Solid Particles from Upper Outlet of Vertical Bubble Columns. *AIChE J.* **1995a**, *41*, 1889−1897.

Hidaka, N.; Onitani, M.; Matsumoto, T.; Morooka, S. Inverted Segregation of Binary Particles in Gas−Liquid−Solid Fluidized Bed. *Powder Technol.* **1995b**, *84*, 157−163.

Hsu, Y. C.; Dudukovic, M. P. Gas Holdup and Liquid Circulation in Air-Lift Reactors. *Chem. Eng. Sci.* **1980**, *35*, 135−141.

Jones, A. G. Liquid Circulation in a Draft-Tube Bubble Column. *Chem. Eng. Sci.* **1985**, *40*, 449−462.

Kubota, H.; Hosono, Y.; Fujie, K. Characteristic Evaluations of ICI Air-Lift Type Deep Shaft Aerator. *J. Chem. Eng. Jpn.* **1978**, *11*, 319−325.

Matsumoto, T.; Hidaka, N.; Morooka, S. Axial Distribution of Solid Holdup in Bubble Column for Gas−Liquid Solid Systems. *AIChE J.* **1989**, *35*, 1701−1709.

Matsumoto, T.; Hidaka, N.; Takenouchi, H.; Morooka, S. Segregation of Solid Particles of Two Sizes in Bubble Columns. *Powder Technol.* **1991**, *68*, 131−136.

Matsumoto, T.; Hidaka, N.; Gushi, H.; Morooka, S. Axial Segregation of Multicomponent Solid Particles Suspended in Bubble Columns. *Ind. Eng. Chem. Res.* **1992**, *31*, 1562−1568.

Merchuck, J. C.; Stein, Y. Local Hold-up and Liquid Velocity in Air-Lift Reactors. *AIChE J.* **1981**, *27*, 377−388.

Popovic, M. K.; Robinson, C. W. The Specific Interfacial Area in External-Circulation-Loop Airlifts and a Bubble Column: 1. Aqueous Sodium Sulfite Solution. *Chem. Eng. Sci.* **1987a**, *42*, 2811−2824.

Popovic, M. K.; Robinson, C. W. The Specific Interfacial Area in External-Circulation-Loop Airlifts and a Bubble Column: 2. CMC/Sulfite Solution. *Chem. Eng. Sci.* **1987b**, *42*, 2825−2832.

Popovic, M. K.; Robinson, C. W. Mass Transfer Studies of External-Loop Airlifts and a Bubble Column. *AIChE J.* **1989**, *35*, 393−405.

Richardson, I. F.; Zaki, W. N. Sedimentation and Fluidization. Part 1. *Trans. Inst. Chem. Eng.* **1954**, *32*, 35−52.

Received for review May 16, 1997
Revised manuscript received September 25, 1997
Accepted September 28, 1997[⊗]

IE970353F

[⊗] Abstract published in *Advance ACS Abstracts*, November 15, 1997.